PROCEDURE FOR PRELIMINARY DESIGN OF OPTIMUM AIRCRAFT STRUCTURES

A. P. C. S. Ferreira, apferre@ita.br
S. F. M. Almeida, frascino@ita.br
Department of Mechanical Engineering, Instituto Tecnológico de Aeronáutica - ITA, CTA-ITA-IEM, Praça Mal. Eduardo Gomes, no 50, São José dos Campos, SP, 12228-900, Brazil

R. C. Gama, renata.gama@embraer.com.br
Empresa Brasileira de Aeronáutica Embraer, São Jose dos Campos, SP, Brazil.

Abstract. *This work presents a new numerical methodology to obtain self-equilibrated load cases from an aircraft load envelope and a robust optimization procedure. The physical non uniform loading is represented by piecewise linear functions defined at a number of arbitrary load control points including parameters that control the robustness of the load representation. The load control points are arbitrarily distributed along the structure edges. A better correlation between the physical loading and its numerical representation is achieved as the number of load control points increases. This new methodology allows the representation of any arbitrary non uniform loading with a prescribed degree of fidelity and robustness. As an example, the obtained load cases are used for the buckling load optimization of an aircraft reinforced panel. The minimax strategy is used in the optimization process: the buckling load is maximized with respect to the geometric properties and minimized with respect to the self-equilibrated load cases. The result is the best geometric properties for the worst load case. A mass optimization external loop is implemented to yield a minimum mass structural design that satisfies the design requirements within a prescribed safety margin.*

Keywords*: non uniform loading, structural optimization, buckling*

1. INTRODUCTION

The aeronautical structures are subjected to a large variety of loadings that result in a large number of complex stress and strain distributions. Therefore, the aeronautical design could be non conservative if the loading is considered to be uniform. On the other hand, the computational cost of the optimization procedure would be prohibitive if hundreds of load cases were taken into account. A good alternative is to determine the critical load cases and use only them in the optimization process.

In order to work with a reduced set of load cases, Elishakoff (1983) proposed to use a probability density function associated with each loading. However, these probability distributions are not always known and it is difficult to mathematically express them.

Another methodology to deal with a reduced set of load cases is the convex method (Bem_haim and Elishakoff, 1990). In this method, a group of critical loadings, similar to the vertices of a convex polygon, is selected. A load space is created with these loadings assuming that all the elements of this load space have equal probability of occurring. Cherkaev and Cherkaeva (1999) used this methodology and proposed a procedure to maximize the buckling load with respect to the thickness of a panel and minimize with respect to the load cases. This methodology yields a robust structure for the load cases applied to it.

The issue of selecting the critical load cases is of utmost importance for the optimization of aeronautical structures. Typically, there are a very large number of load cases to be accounted for. Elishakoff (1983), Ben_haim and Elishakoff (1990) and Cherkaev and Cherkaeva (1999) present some interesting approaches to deal with this problem but they do not address some important aspects of the problem. For example, the actual load cases of an aircraft component are always self equilibrating as the component may be assumed to be in static equilibrium. Moreover, unlike the typical assumption used in most optimization works, they are typically non uniform along the edges of the plates due to stiffness variation along the component. Therefore, the load distribution usually changes as the optimization procedure changes the design variables (dimensions of the parts). This problem is very complex and a robust procedure needs to be developed to account for this fact.

The methodology to represent the load cases proposed in this work is based on the work developed by Conrado et al. (2005). It represents non uniform loadings by piecewise linear functions defined along the boundary of the structure using loading control points. Assuming that the component is under static equilibrium the non uniform loadings should be self-equilibrated. Moreover, in this case the buckling modes are not affected by the position of the imposed constraints to prevent rigid body movement. However, in the work developed by Conrado et al. (2005), the obtained self-equilibrated loadings have no correspondence to the physical loadings applied to the structure. Moreover, as they are self equilibrated, they have no magnitude. So, optimizing a structure based on the loadings obtained from the procedure developed by Conrado et al. (2005) implies in getting an optimal structure considering load cases that possibly will not occur in practical situations resulting in an over dimensioned design.

The present work describes a procedure that relates the physical loading to the self-equilibrated loadings. Parameters that control the design robustness with respect to each physical loading at each load control point were also included in the formulation. Therefore, the optimum panel is obtained considering a set of physical load cases chosen to represent the main load cases applied to the structure. This modification makes the load representation closer to real situations and the robustness of the design may be arbitrarily prescribed.

An important additional advantage of this methodology is that it takes advantage of the fact that many aircraft structures are statically determinate. For example, one can compute exactly the moment distribution on a wing based on the pressure distribution obtained from an aerodynamic analysis. These moments are independent on the stiffness distribution of the wing structure but they can be used to compute integrals of the internal forces along the edges. This information can be used to define the magnitude of the considered self equilibrated load cases. In this way, the obtained non uniform loading representation does not depend on the structural stiffness distribution. This feature is suitable for optimization problems since the structural stiffness is continuously modified during the optimization process.

The optimization of the panel geometric properties under the load cases that represents the physical loads is done using the minimax strategy, as used in Faria and Almeida (2003). In this work, the minimax strategy goal is to get maximum buckling for the worst loading condition. The objective function is minimized with respect to the loading cases and maximized with respect to the design variables. A mass optimization external loop is implemented to yield a minimum mass structural design that satisfies the design requirements within a given safety margin.

The structure chosen for optimization is an isotropic panel with two reinforcers. The optimization algorithm is implemented in a Fortran code and software Abaqus© is used for buckling computation. Using Abaqus© associated with a Fortran code makes the optimization procedure proposed in this work more flexible and general. The procedure can be easily adapted for the linearized buckling optimization of any type of aeronautical structure. Also, the analysis is more reliable using commercial software such as Abaqus©.

2. NON UNIFORM LOADING REPRESENTATION

The basic data required for the non uniform loading representation is the shear and compressive stresses on a panel of an aircraft wing. These stresses are originated from the vertical resultant forces distributions, bending and torsional moment distributions on the wing, which are originated from the wing pressure distribution. Figure (1) depicts the steps for computing the compressive and shear stress resultants on a wing panel. Considering that the aircraft wing is in static equilibrium the forces and moments distributions will not depend on the stiffness distribution of the wing. The same holds for the resultant shear and compressive stresses on the panels.

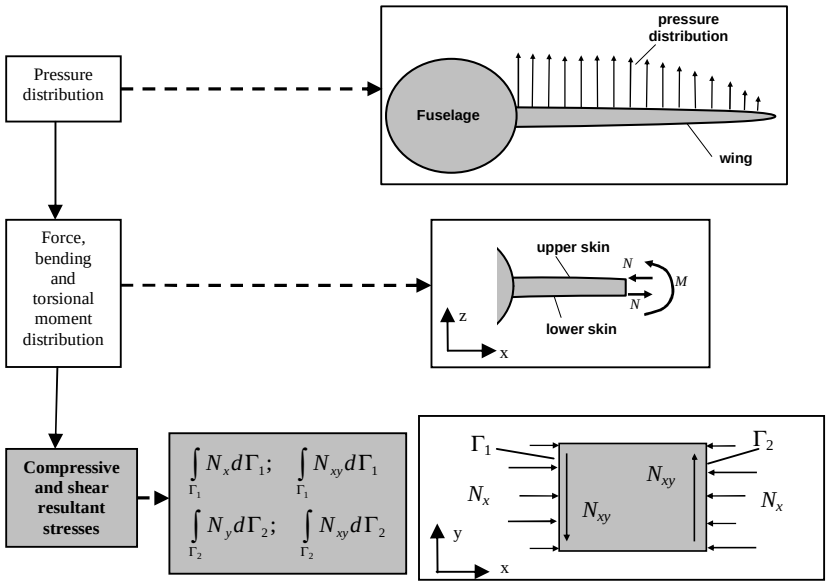

Figure 1. Compressive and shear resultant stresses.

As an example, suppose that the bending moment at a certain point along the wing is known from an aerodynamic analysis. Considering that the wing is in pure bending, the load corresponding to the integral of the stress resultant can be easily estimated independent on the stiffness distribution of the wing. Therefore, the magnitude of the self

equilibrating loading cases can be determined by imposing that their integral along this edge are the load computed from the bending moment. Naturally, an arbitrary number of additional constraints may be imposed on the self-equilibrated loading cases if the complexity of the physical load case requires.

This work assumes that the resultant shear and compressive stresses on the panel are known. Therefore, the first step of the non uniform loading representation is to perform the compressive and shear load discretization. These loads are assumed to be discretized by piecewise linear functions distributed along the edges of the structure. Figure (2) depicts a non uniform load distribution applied to a structure edge and the corresponding load discretization.

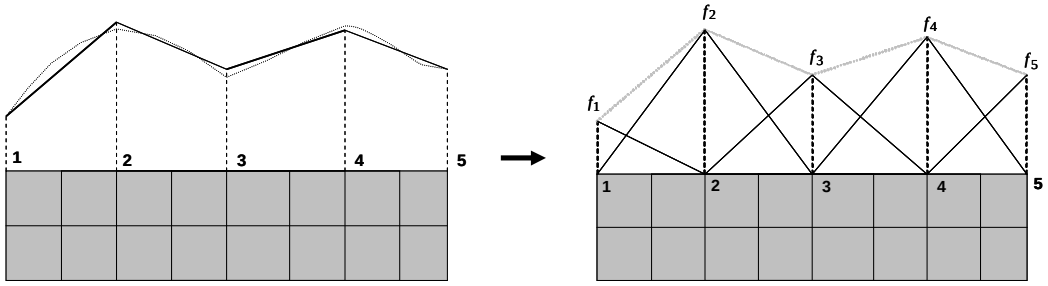

Figure 2. Load discretization.

In Fig. (2), points 1, 2, 3, 4, and 5 are defined as load control points; in these points the magnitude of the loads are prescribed. The number and position of the load control points are arbitrary. They are chosen based on trade off between computational cost and accuracy of physical load representation. As a general rule, in order to consider the load transfer mechanisms, the structure must have two coincident load control points at each corner (to account for loads discontinuities between the edges) and one near each reinforcement end (to account for load variation due to sudden variation of stiffness). The loads magnitudes are defined by the loading parameters f_1, f_2, f_3, f_4 and f_5 in Fig. (2). Load parameters f_i may be either loads along the x or y directions. Therefore, for a two dimensional problem, at each load control points correspond two loading parameters.

After defining the loading discretization, it is necessary to enforce constraints in the finite element model to preclude rigid body motion. In the two dimensional case presented as an example in this work, if suffices to constrain the displacements of two nodes along the x direction (these two nodes must not have the same y coordinate) and one along the y direction to preclude rigid body motion in the xy plane. These boundary conditions do not cause spurious reaction loads when self equilibrating load cases are considered.

In fact, if one considers an aircraft component under static equilibrium, all resulting load distribution are self equilibrating. Since the load distribution must be self equilibrating, the equilibrium conditions of forces along x and y directions and moments along the z axis must be satisfied. Of course, these equations apply only for the two dimensional case presented herein. For the three dimensional case there would be six equations of equilibrium. The loading magnitudes at the load control points are the unknown in this system of equations described in Eq. (1):

$$\begin{aligned} \sum F_x &= 0 \\ \sum F_y &= 0 \\ \sum M_0 &= 0 \end{aligned} \tag{1}$$

The equilibrium equations can now be rewritten in matrix form as:

$$[G]\{X\} = \{0\} \tag{2}$$

where $[G]$ is $3\times m$ matrix, m is two times the number of loading control points, corresponding the x and y components at each load control point. $\{X\}$ is the loading magnitude vector containing the load magnitude at each load control point. Matrix $[G]$ and vector $\{X\}$ are given, respectively, by:

$$[G] = \begin{bmatrix} I_1 + J_1 & 0 & I_2 + J_2 & 0 & \cdots & I_{m/2} + J_{m/2} & 0 \\ 0 & I_1 + J_1 & 0 & I_2 + J_2 & \cdots & 0 & I_{m/2} + J_{m/2} \\ -(N_1 + O_1) & T_1 + U_1 & -(N_2 + O_2) & T_2 + U_2 & \cdots & -(N_{m/2} + O_{m/2}) & T_{m/2} + U_{m/2} \end{bmatrix} \tag{3}$$

where the terms I_i, J_i, K_i, L_i, N_i, O_i, T_i and U_i represent the contribution of the loading distribution.

$$\{X\}^T = \begin{bmatrix} f_{x_1} & f_{y_1} & f_{x_2} & f_{y_2} & \dots & f_{x_{m/2}} & f_{y_{m/2}} \end{bmatrix} \tag{4}$$

It is possible to see that the number of unknowns is greater than the number of equations in Eq. (2). Conrado et al. (2005) dealt with this numerical problem, minimizing the following function to obtain the self-equilibrated loadings:

$$e = \left(\{n\}^T - \{X\}^T\right)\left(\{n\} - \{X\}\right) \tag{5}$$

where $\{n\}$ is an unit base vector. For example, $\{n_1\}^T = \{\ 1\ \ 0\ \ 0 \dots 0\ \}$. In this case Eq. (2) is used as a constraint to the problem and vector $\{X\}$ is obtained according to the following equation:

$$\{X\} = \left([I] - [G]^T\left([G]\ [G]^T\right)^{-1}[G]\right)\{n\} \tag{6}$$

since $\{n\}$ can be m different vectors, it is possible to get m different vectors of load magnitudes $\{X\}$ that are self-equilibrated load cases. Since, the self equilibrating loads do not have magnitude, in Conrado et al. (2005), for each self-equilibrated load case, one optimization process is performed to obtain the optimum design to establish the maximum magnitude for this load case. This value is used to define the magnitude for each self equilibrated loading. This procedure makes the computational cost high and the resulting design may be very conservative because, in practical situations, not all of these loads will occur simultaneously. Furthermore, the magnitude definition described above for each self-equilibrated load cases is not related to the physical loads that act on the structure.

Aiming at bringing the structural optimal design closer to real situations, this work proposes some changes in the approach of obtaining self-equilibrated load cases used in Conrado et al (2005). The idea is to define magnitudes for the self equilibrated loadings that represent each actual physical load within the load envelope of the structure and provide parameters that control de robustness of the optimization procedure.

Therefore, the null vector in Eq. (2) is replaced by vector $\{A\}_j$ which is null in the first three rows defining the equilibrium conditions and have the physical load magnitudes in the others rows. The index j refers to the load case considered. This vector makes possible to get a self-equilibrated loading case that corresponds to a physical one. Moreover, this approach can provide a meaningful definition of self equilibrated loading with very little computational cost. The $[G]$ matrix in Eq. (2) is replaced by a $[\bar{G}]$ matrix which includes extra rows. The first three rows still representing the sum of forces and moments, the others lines represent the forces on the edges where the physical loads are applied:

$$[\bar{G}]\{X\} = \{A\}_j \tag{7}$$

In this new methodology the function that should be minimized to solve Eq. (7) is also modified. Here Eq. (7) is used as a constraint on the function in Eq. (8) minimization:

$$e_j = \left(p_{ij}\bar{\mathrm{F}}_{\mathrm{ij}}\{n\}_j^T - \{X\}_j^T\right)\left(p_{ij}\bar{\mathrm{F}}_{\mathrm{ij}}\{n\}_j - \{X\}_j\right) \tag{8}$$

where p_{ij} is a dimensionless parameter arbitrarily chosen in the range [0, 1]. These parameters define the load magnitude percentage applied at each load control point. The subscript j refers to the load case considered and i refer to the load control point. This parameter p_{ij} provides the designer with the capability of choosing whether the physical load representation should be conservative or not. If p_{ij} is chosen to be 1 the load magnitude at load control point i corresponding to the j-th physical load will tend to be very conservative, as in Conrado et al. (2005). On the other hand, if it is chosen to be zero the load magnitude at load control point i corresponding to the j-th physical load will tend to be very non-conservative. Typically, from the design point of view it is interesting to use a value between these two limits.

$\bar{F}_{ij}$ is the magnitude of the load applied at the load control point. It is defined from the load applied on the edge where load control point is located:

$$\bar{F}_{ij} = \frac{2\ A}{\int_{i-1}^{i}\sqrt{\left(\frac{dx}{ds}\right)^2 + \left(\frac{dy}{ds}\right)^2}\,ds + \int_{i}^{i+1}\sqrt{\left(\frac{dx}{ds}\right)^2 + \left(\frac{dy}{ds}\right)^2}\,ds} \tag{9}$$

where A is the load applied on the edge considered. The solution of this minimization problem yields vector $\{X\}_j$:

$$\{X\}_j = \left([I] - \left[\bar{G}\right]_j^T \left(\left[\bar{G}\right]_j \left[\bar{G}\right]_j^T \right)^{-1} \left[\bar{G}\right]_j \right) p_{ij} \bar{F}_{ij} \{n\}_j + \left[\bar{G}\right]_j^T \left(\left[\bar{G}\right]_j \left[\bar{G}\right]_j^T \right)^{-1} \{A\}_j \tag{10}$$

Vector $\{X\}_j$ is the self-equilibrated load case j corresponding to the physical load case j. In this way, having the load envelope of a structure, it is possible to optimize it for the specific load envelope. This procedure reduces the computational cost and leads to a more efficient and robust design.

3. OPTIMIZATION STRATEGY

The minimax strategy (Dem'yanov and Malozemov, 1974) is defined by Eq. (11). It is used in this work with the goal of getting the best design for the worst load condition:

$$\max_{\{t\}} \min_{\{\beta\}} (\lambda(\{t\},\{\beta\}) = \max_{\{t\}} \phi(\{t\}) \quad , \quad \phi(\{t\}) = \min_{\{\beta\}} (\lambda(\{t\},\{\beta\}) \tag{11}$$

In the first part of the minimax strategy the objective function is minimized with respect to load cases $\{\beta\}$ by a random search. In the second part of the minimax strategy the objective function is maximized with respect to the design variables $\{t\}$. This is done by Powell's method (Vanderplaats, 1984 and Powell, 1964) which is a traditional zero order optimization method. Geometric constraints were included in the optimization algorithm to guarantee that the search was performed only in the feasible region.

An external mass optimization loop is included in the optimization process to minimize the structural weight satisfying the design requirements. This external loop was used in a previous work (Ferreira et al, 2009) with satisfactory results. The complete optimization process is represented in the diagram of Fig. (3).

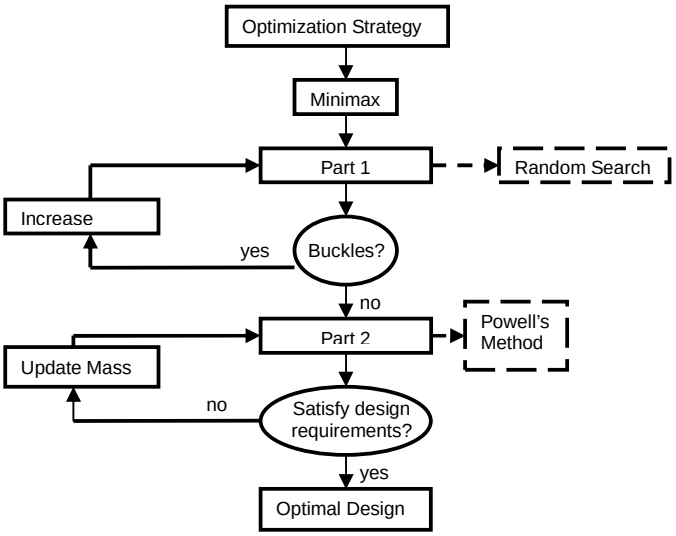

Figure 3. Optimization process diagram.

It can be seen from the optimization diagram that by the end of the first part of the minimax strategy it is verified whether the considered structure buckles or not. If it buckles, the structure mass should be increased and first part is repeated until a not buckled structure is obtained. The verification whether the structure is under or over dimensioned is performed at the end of the second part of the minimax strategy. If the structure satisfies the safety margins and design requirements, the optimization process is completed. If not, the mass should be updated and part two of the optimization process repeated.

One important issue is estimation of the required mass correction. An inappropriate mass adjustment factor can result in an optimization process that does not converge. The mass adjustment factor used in this work varies with the cubic root of the buckling optimal load. The theoretical base for this mass adjustment factor is that the flexural structural stiffness varies with the cube of the thicknesses for flat plates. This factor is not exact for the structure optimized in this work because of the flexural stiffness of the reinforcements. However, it represents a good approximation.

4. NUMERICAL RESULTS

The structure chosen for optimization is a rectangular isotropic plate with two reinforcers as represented in Fig. (4). The plate dimensions are 0.4 m in the *y* direction and 1.2 m in the *x* direction. The material is aluminum with Young modulus of 70 GPa, mass density of 2600 kg/m^3 and Poisson ratio 0.3. The reinforcers are positioned at $x = 0.4$ m and $x = 0.8$ m, dividing the plate in three sections. The design variables are defined for obtaining a symmetric structure. In this way, the width and height of the two reinforces comprise two design variables ($w_1 = w_2$ and $h_1 = h_2$) and the three sections comprise another two design variables ($t_1 = t_3$ and t_2). Figure (4) depicts the reinforced panel with its design variables. A base plate is used to avoid null values for the design variables. The same is done with the reinforcers width and height values. Since the magnitudes of the sections thicknesses and reinforcers width and height can be significantly different, the design variables must be normalized in the optimization process.

The load control points are positioned according to Fig. (5). It was assumed that the load envelope is composed of five load cases. Table 1 describes the considered load cases. In Tab. 1, the symbol "×" means that a load at an edge is present; the total force represents the value of the integral of the force over the prescribed edges.

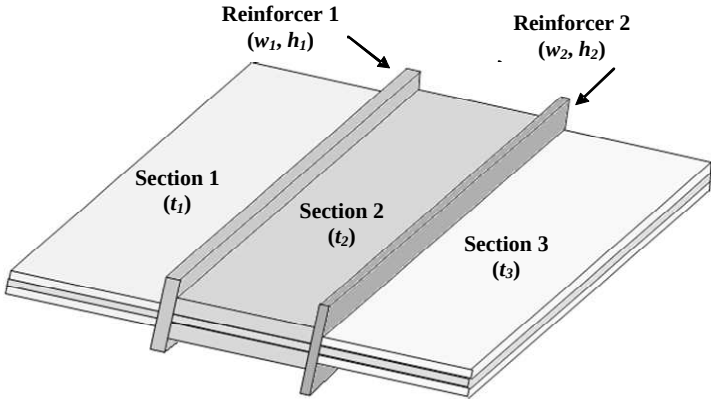

Figure 4. Design variables.

Table 1. Load cases.

Segments	Case 1 compression	Case 2 compression	Case 3 shear		Case 4 compression	Case 5 shear	
A	×		×				
B	×		×				
C	×		×				
D							
E					×	×	
F					×		
G					×		×
H		×		×			
Total Force (*N*)	*3600*	*500*	*-1200*	*1200*	*2800*	*-880*	*720*

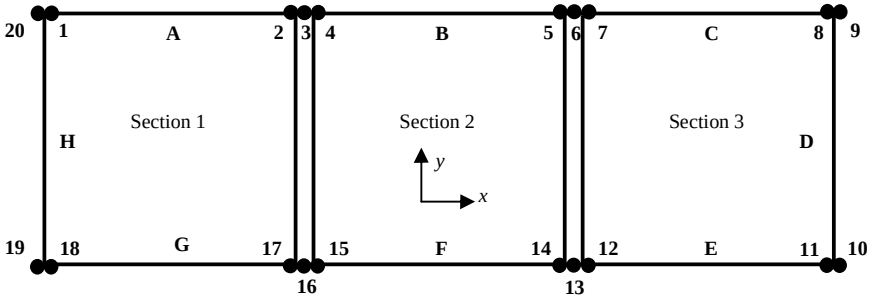

Figure 5. Load control points positions.

The finite element model to compute the buckling load was implemented using Abaqus©. It was used 240 shell elements for the panel and 10 beam elements for each reinforcer.

This work presents three examples of panel optimization, the difference among them is the loading applied. The first example uses $p_{ij} = 0$ in Eq. (10). The second example uses $p_{ij} = 1$ and the third uses $p_{ij} = 0.25$.

4.1. Reinforced panel considering $p_{ij} = 0$

In this work, twenty load control points were used. This quantity is justified by the necessity of placing load control points near the reinforcers to account for the load distribution variation due to the stiffness variation. From the load control points distribution, Fig. (5), and plot of Force × Edge distance, Fig. (6), it can be seen that at points 3, 6, 13 and 16 the load magnitude is significantly lower because the segments length defined by these points are smaller compared to the others. So, their contribution to the force sum at the edge is small. If at the physical load being considered there are significant loads at these points, it would be necessary to create a new self-equilibrated load vector for the load control point considered using $p_{ij} \neq 0$. Furthermore, the self-equilibrated loading obtained when p_{ij} is equal to zero is almost uniformly distributed. This is not a realistic load representation since physical loads are non-uniformly distributed.

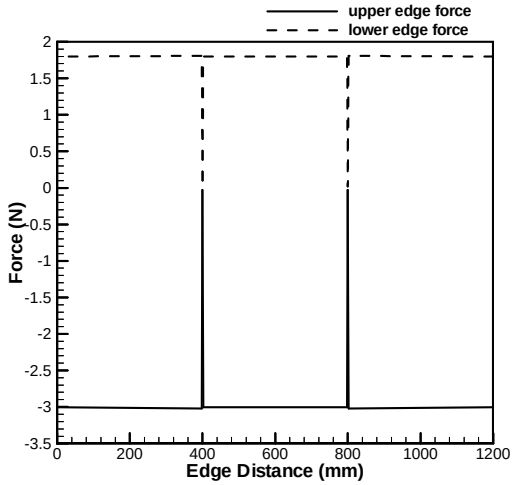

Figure. 6 Self-equilibrated loading for load case 1, $p_{ij} = 0$.

Table 2. Optimization results $p_{ij} = 0$.

	Initial Structure 1		Initial Structure 2		Initial Structure 3	
	Initial (*mm*)	Optimum (*mm*)	Initial (*mm*)	Optimum (*mm*)	Initial (*mm*)	Optimum (*mm*)
t_1	2.5	1.18	3.8	1.17	3.8	1.16
t_2	2.5	1.18	1.2	1.14	1.07	1.17
w_1	4	4	3	4	4	4
h_1	80	10.25	42	14.36	34.13	11.57
mass *(kg)*	3.76	1.55	3.9	1.56	3.9	1.54
λ_1	9.94	1.02	1.32	1.00	0.94	1.00
λ_2	25.40	2.67	6.62	2.63	4.66	2.57
λ_3	19.01	1.93	2.93	1.95	2.06	1.88
λ_4	12.78	1.31	1.70	1.29	1.20	1.29
λ_5	14.67	1.53	1.79	1.44	1.26	1.52

Table 2 presents the optimization results for the reinforced panel under the load cases described in Tab. 1.The optimization is performed for three different initial structures. The first and the second initial structures are over dimensioned for the load cases considered. They support loads that are almost ten times and 32% larger than the ones that are actually applied, respectively. The third initial structure is under dimensioned, that is, it buckles under the

considered load cases. The buckling load is defined by λ. The used stop criterion for the optimization was 2%, that is, the optimization stops when the normalized objective function is in the range [1.00 – 1.02].

Analyzing Tab. 2 it is concluded that the load case 1 was the critical one resulting in the lowest buckling values before and after the optimization process. Using the mass optimization external loop, the three initial structures converged to design variables that satisfy the design requirements and safety margins. However, optimal structure 3 can be considered the best since its mass is the lowest among the three optimal structures.

4.2. Reinforced panel considering $p_{ij} = 1$

Setting p_{ij} = 1 in Eq. (10) corresponds to assume that the entire edge load given by $\{A\}_j$ is concentrated at load control point *i*. In order to compute the self-equilibrated loading, it is first necessary to determine the force magnitude at the load control point *i*, given by $p_{ij}\overline{F}_{ij}$. Seven self-equilibrated load cases were obtained by using the methodology described in Section 2. The first three self-equilibrated load cases were obtained using load case 1 and p_{ij} = 1 at load control points 2, 5 and 8. This loading definition was adopted because it was concluded in Subsection 4.1 that the load case 1 is the critical one. The others four self-equilibrated load cases are load cases 2 to 5 with p_{ij} = 0. Figure 7 presents the self-equilibrated loading for load case 1 and load control point 2 and Tab. 3 presents the optimization results.

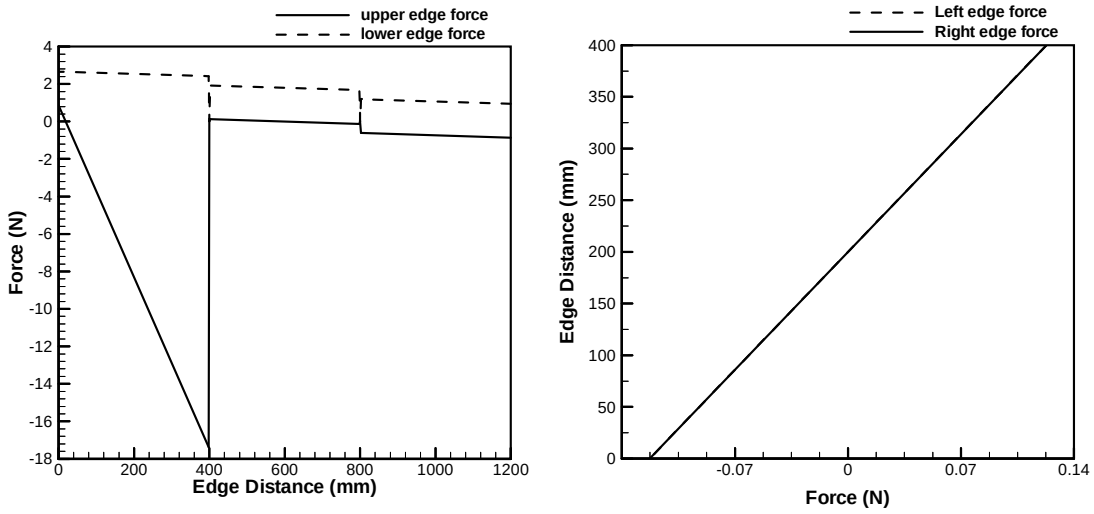

Figure 7. Self-equilibrated loading for load case 1 and load control point 3, p_{21} = 1.

Table 3. Optimization results p_{ij} = 1.

	Initial Structure 1		Initial Structure 2		Initial Structure 3	
	Initial (*mm*)	Optimum (*mm*)	Initial (*mm*)	Optimum (*mm*)	Initial (*mm*)	Optimum (*mm*)
t_1	2.5	1.51	3.8	1.51	3.8	1.51
t_2	2.5	1.61	1.2	1.66	1.07	1.66
w_1	4	4	3	3.08	4	4
h_1	80	18.32	42	21.64	34.13	18.40
mass (*kg*)	3.76	2.07	3.9	2.08	3.9	2.09
λ_1	4.75	1.01	2.43	1.00	1.72	1.00
λ_2	4.01	1.02	0.48	1.08	0.34	1.11
λ_3	4.69	1.03	2.76	1.02	1.95	1.01
λ_4	25.40	5.67	6.62	5.63	4.66	5.59
λ_5	19.01	4.19	2.93	4.17	2.06	4.13
λ_6	12.78	2.91	1.70	2.85	1.20	2.90
λ_7	14.67	3.77	1.79	3.86	1.26	4.09

When, for example, parameters p_{21} is equal to one, it can be observed from the load control point distribution (Fig. (5)) and Force × Edge distance plots (Figs. (7)) that there is a large load concentration at section 1 at the upper edge. Physical loadings with such a load concentration are not common and the structure designed to support these loadings will probably be over dimensioned for practical applications.

It is concluded from Tab. 3 that load case 1 is critical. For this case, the lowest buckling loads result before and after the optimization process. Optimal structure 1 has the lowest mass, so it can be considered the global optimum. Using the mass optimization external loop, the three initial structures converged to design variables that satisfy the design requirements and safety margins. Consistently, the mass of the optimal structures for $p_{ij} = 1$ are larger than the ones obtained when $p_{ij} = 0$. This is expected since the load representation when $p_{ij} = 1$ is more concentrated and non-uniformly distributed.

4.3. Reinforced panel considering $p_{ij} = 0.25$

Using the five physical load cases results in 32 self-equilibrated load cases for $p_{ij} = 0.25$ at all load control points. Load case 1 is a compressive load acting at the edge with load control points 1 to 8; choosing $p_{ij} = 0.25$ at each one; eight self equilibrated load cases result. Load case 2 is a compressive load acting at the edge with load control points 19 and 20; this yields another two self-equilibrated load cases. Load case 3 is a shear load defined at the edge with load control points 1 to 8 and at the edge with load control points 19 and 20; this results in another ten self-equilibrated load cases. Load case 4 is a compressive load at edge with load control points 11 to 18 yielding another eight self equilibrated load cases. Load case 5 is a shear load defined at the edge with load control points 11 and 12 and on the edge with load control points 17 and 18; this results in another four self equilibrated load cases.

Figure (8) presents the plots of Force × Edge distance when p_{21} is equal to 0.25. The comparison between the load distribution using p_{ij} equal to one and the load distribution using p_{ij} equal to 0.25, can be made by comparing the load control point distribution presented in Fig. (7) and Fig. (8). There is also load concentration at section 1 at upper edge, when parameter p_{21} is equal to 0.25. However, this load concentration is smaller than the one that happens when p_{ij} is equal to one. The overall load distribution in these cases is more typical of non-uniform physical loading. The structure designed to support these loadings will probably support a large variety of loadings that are present in practical applications.

Analyzing Tab. 4 it is observed that the load case 1 is critical load case. It yields the lowest buckling loads before and after the optimization process. Optimal structures 2 and 3 have the same mass (lower than optimal structure 1) and almost the same shape. Therefore, these two structures are the best ones. Using the mass optimization external loop, the three initial structures converged to design variables that satisfy the design requirements and safety margins. The mass of the optimal structures has an intermediate value compared to the ones obtained for $p_{ij} = 0$ and $p_{ij} = 1$. This is consistent with the fact that the loading represented by $p_{ij} = 0.25$ is not as concentrated as the one represented by $p_{ij} = 1$ and also not uniformly distributed as the one represented by $p_{ij} = 0$.

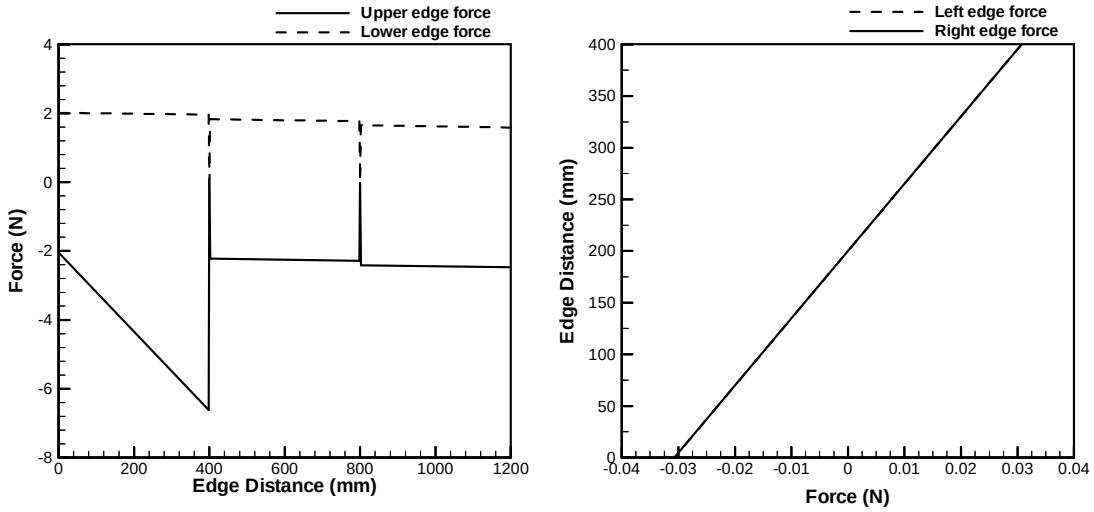

Figure 8. Self-equilibrated loading for load case 1 and load control point 3, $p_{21} = 0.25$.

Table 4. Optimization results p_{ij} = 0.25.

	Initial Structure 1		Initial Structure 2		Initial Structure 3	
	Initial (*mm*)	Optimum (*mm*)	Initial (*mm*)	Optimum (*mm*)	Initial (*mm*)	Optimum (*mm*)
t_1	2.5	1.28	3.8	1.28	3.8	1.25
t_2	2.5	1.32	1.2	1.31	1.07	1.29
w_1	4	2.48	3	3.73	4	4
h_1	80	17.59	42	12.00	34.13	14.5
mass (*kg*)	3.76	1.70	3.9	1.69	3.9	1.69
λ_1	8.21	1.04	1.81	1.05	1.28	1.02
λ_2	8.19	1.02	1.55	1.02	1.09	1.01
λ_3	10.27	1.29	1.33	1.33	0.94	1.33
λ_4	7.56	1.00	0.93	1.00	0.66	1.01
λ_5	7.56	1.00	0.93	1.00	0.66	1.01
λ_6	10.27	1.29	1.33	1.33	0.94	1.33
λ_{32}	14.65	1.96	1.79	2.04	1.26	2.02

5. CONCLUSION

The methodology proposed in this work makes possible to extract self-equilibrated load cases with magnitude associated with physical load cases within an arbitrary prescribed accuracy. The load representation is more realistic and the resulting designs robustness can be adjusted using parameters p_{ij}. If these values are close to zero the self equilibrated loadings tend to be almost uniform. If the values are close to one, self equilibrated loadings tend to be more concentrated. Therefore, these parameters must be judiciously chosen by the designer to obtain a realistic load representation and, consequently, yield an optimal design that has a reasonable safety margin.

In the examples presented the mass of the optimal structure were larger for larger values of parameters p_{ij}. This confirms the p_{ij} parameters ability to define the degree of robustness of the optimal design. That is, if p_{ij} are equal to one, the loading is considered almost concentrated and the optimum structure must be heavier to support this unrealistic loading; therefore, the design is very conservative. If p_{ij} are equal to zero, the considered loads are almost uniform and the optimum structure is lighter. But, the optimal design tends to be non conservative because non-uniform loads typically exist in practical applications. When p_{ij} are set equal to 0.25, the considered loading non-uniform and the optimal structure mass has an intermediate value. Since the loading representation with p_{ij} = 0.25 is more realistic, it is possible to state that, for the studied example, the corresponding optimal structure would have better performance in practical application.

Parameters p_{ij} were shown to control the robustness of the design. In this work, these parameters were only considered to be 0, 0.25 or 1.0 to demonstrate this feature. But it must be emphasized that those parameters can be chosen for each load control point for each particular load case. Therefore, these parameters offer valuable flexibility to the designer but there is a need to establish guidelines for their choice. The development of a general and realistic representation of non-uniform loadings will be the subject of a future work. This will include a procedure to select the number of load control points and the value of the p_{ij} parameters according to the nature of each particular applied physical load.

The optimization using the minimax strategy makes possible to obtain the best design and identify the worst loading condition. In all cases tested the critical buckling load was maximized and the mass reduced.

In summary, the proposed methodology can efficiently yield optimum structures under arbitrary non-uniform loadings. Moreover, the accuracy of the load representation and the robustness of the design can be arbitrarily prescribed. Therefore, this tool can be extremely valuable for the preliminary design of aircraft structures.

6. ACKNOWLEDGEMENTS

This work is financed by the Brazilian Agencies FAPESP (Grant No. 06/60929-0) and CNPq (Grant No. 305601/2007-5).

7. REFERENCES

Ben_haim, Y, Elishakoff, I., 1990. “Convex Models of Uncertainly in Applied Mechanics”. Elsevier science publisher, New York.

Cherkaev, G., Cherkaeva, A., 1999. “Optimal design for uncertain loading condition”, in: Berdichevsky, V., Jikov, V., Papanicolau G. (Eds.), Homogenization. World scientific, Singapore, pp. 193-213.

Conrado, A. C., Faria, A. R., Almeida, S. F. M., 2005. “Optimum design for buckling of arbitrary shaped ribs under uncertain loadings”. The Aeronautical Journal, 109, 609-618.

Dem’yanov, V. F., Malozemov, V. N., 1974. “Introduction to Minimax”. John Wiley & Sons, New York.

Elishakoff, I., 1983. “Probabilistic Methods in the Theory of Structures”. Wiley Interscience, New York.

Faria, A.R, Almeida, S. F. M., 2003. “Buckling optimization of plates with variable thickness subjected to nonuniform uncertain loads”. International Journal of Solids and Structures. 40, 3955-3966.

Ferreira, A. P. C. S., Faria, A. R., Almeida , S. F. M., 2009. “Simultaneous buckling and fundamental frequency optimization of composite plates under uncertain loadings”. Proceedings of the 17th International Conference on Composite Materials (ICCM-17), Edinburgh, Scotland.

Powell, M. J. D., 1964. “An efficient method for finding the minimum of a function of several variables without calculating derivatives”. Computer Journal. 7, 155-162.

Vandeplaats, G., 1984. “Numerical Optimization Techniques for Engineering Design: With Application”. McGraw-Hill, New York.

8. RESPONSIBILITY NOTICE

The authors are the only responsible for the printed material included in this paper.